IEEE Robotics and Automation Letters (RA-L) paper, presented at ICRA 2026, Vienna, Austria. Cite as RA-L paper.

Robotic Exoskeleton With Mechanically Implemented Kinematic Synergy for Quadrupedal Gait of Rats

Takayuki Miyamoto, *Graduate Student Member, IEEE*, Andrey Mikhailov, Modar Hassan, *Member, IEEE*, Sandra Puentes, *Member, IEEE*, Taichi Hiraga, Hideaki Soya, and Kenji Suzuki, *Senior Member, IEEE*

***Abstract*—This study introduces a novel kinematic synergy-based exoskeleton designed for gait rehabilitation studies in rats. The exoskeleton assists all three hindlimb joints of the rat (hip, knee and ankle) while ensuring proper interjoint coordination and the natural quadrupedal posture. This assistance is realized through a 2-DOF bar mechanism that emulates the biomechanics of rats. Engineered to be compact, lightweight, backdrivable, and sufficiently powerful, the proposed system minimizes physical stress on the animal while allowing a wide range of assistive forces to be applied. These features are achieved through a combination of a cable power transmission system and direct-drive motors positioned outside the exoskeletal structure. The desktop experiments demonstrated that the exoskeleton could precisely replicate the rat's kinematic gait patterns and remain backdrivable whether powered or unpowered. The feasibility of gait assistance was further confirmed in an anesthetized rat, where synergistic gait patterns were observed between the joints. Hence, the system holds the potential to enable controlled comparative neurorehabilitation studies in rats. These studies can help unveil neural recovery mechanisms and design optimal exoskeleton control strategies for rehabilitation in humans.**

***Index Terms*—Rehabilitation robotics, prosthetics and exoskeletons, actuation and joint mechanism, tendon/wire mechanism.**

I. Introduction

LOWER-LIMB robotic exoskeletons with various control strategies have been incorporated into recent physical therapy as a new gait training modality for patients with neurological conditions such as spinal cord injury (SCI), stroke and others [1], [2], [3]. Over the years, numerous studies have investigated the efficacy and efficiency of robot-assisted rehabilitation. Several randomized controlled trials have shown that robotic intervention provides superior motor recovery in patients with paraplegia [4], [5] and stroke patients with upper limb paralysis [6]. In contrast, other studies on lower and upper limb training reported little to no difference in functional improvement between robot-assisted and conventional protocols [7], [8]. Within this limited amount of studies in the field, the concrete advantages of robot-assisted rehabilitation have yet to be unveiled [9], [10], let alone the comparative effectiveness of control strategies [11]. Further, the evaluation methods of these studies are limited to non-invasive measurements as the subjects are human patients, leading to another hindrance to obtaining deeper insights into neural recovery mechanisms.

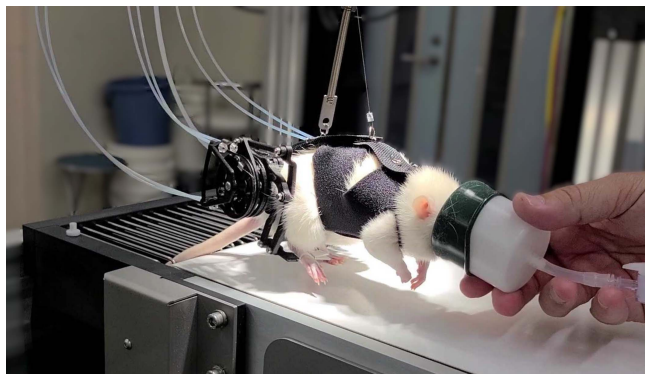

Fig. 1. Proposed exoskeleton having an anesthetized rat walk on the treadmill.

A promising approach to better investigate the impact of robotic intervention is to conduct studies on animals instead of humans. Researchers attempted to develop rehabilitation systems for rats that assist the hindlimbs. There are approaches of assistance: nerve stimulation and physical assistance. In the first approach, researchers reported a drastic improvement in motor functions in rats with SCI and stroke using epidural electrochemical stimulation [12], [13]. Others utilized the peripheral electrical stimulation method and achieved muscle control in anesthetized rats [14]. While these methods focus on cellular/molecular level functionality, this approach leaves room for more precise limb movement control. In the second approach, researchers proposed gait-assistive robotic systems via physical interaction similar to most human rehabilitation devices. Nessler

Received 9 October 2024; accepted 14 January 2025. Date of publication 3 February 2025; date of current version 6 March 2025. This article was recommended for publication by Associate Editor Mahdi Haghshenas-Jaryani and Editor Pietro Valdastri upon evaluation of the reviewers' comments. This work was supported by JSPS KAKENHI under Grant 23KJ0277 and Grant 23H00485. *(Corresponding author: Kenji Suzuki.)*

This work involved human subjects or animals in its research. Approval of all ethical and experimental procedures and protocols was granted by the Animal Research Committee of the University of Tsukuba under Approval No. 24-412, and performed in line with the Fundamental Guidelines for Proper Conduct of Animal Experiments issued by the Ministry of Education, Culture, Sports, Science and Technology (MEXT).

Takayuki Miyamoto is with the PhD Program in Empowerment Informatics, University of Tsukuba, Ibaraki-ken 305-8573, Japan.

Andrey Mikhailov, Modar Hassan, Sandra Puentes, Hideaki Soya, and Kenji Suzuki are with the Center for Cybernics Research, University of Tsukuba, Ibaraki-ken 305-8573, Japan (e-mail: kenji@ieee.org).

Taichi Hiraga is with the PhD Program in Physical Education, Health and Sport Sciences, University of Tsukuba, Ibaraki-ken 305-8573, Japan.

This article has supplementary downloadable material available at https://doi.org/10.1109/LRA.2025.3537858, provided by the authors.

Digital Object Identifier 10.1109/LRA.2025.3537858

IEEE Robotics and Automation Letters (RA-L) paper, presented at ICRA 2026, Vienna, Austria. Cite as RA-L paper.

et al. developed a backdrivable robotic platform consisting of robotic arms and a sliding platform with embedded direct-drive (DD) motors [15], [16]. Florez et al. developed soft rehabilitative exoskeletons for rats using pneumatic actuators [17]. Similarly, Chang et al. developed a wearable device with pneumatic pouch motors [18]. These systems allow safe interaction with the animal's tissues utilizing backdrivable/compliant actuation. However, one common issue is the posture imposed on the animal, which lifts it to an upright posture instead of the innate quadrupedal posture. Such assistance might create ill-trained gait patterns, making the post-training evaluation of the locomotor ability inaccurate. To address this problem, researchers introduced robotic systems that enable quadrupedal locomotion for rats. Song et al. reported the interactive exoskeleton, which allows free overground locomotion with a compact and lightweight configuration and admittance-controlled backdrivability [19]. With similar motivation, Anopas et al. introduced a robotic arm device to enable quadrupedal locomotion [20]. However, they have not considered the backdrivability to the best of our knowledge. While all the robotic systems above enabled gait assistance with dexterous features, none provided physical ankle assistance. Unlike humans, the rat's ankle flexion/extension occurs in a much larger range of motion and plays a more crucial role when generating gait propulsion force against the ground [21]. Hence, ankle assistance is a significant factor in restoring locomotor ability for rats. Although Xi et al. achieved joint control including ankles with electrical stimulation, physical assistance can provide better-coordinated kinematics and may broaden the variety of experiments through different sensory inputs to the bio-system [14].

In this letter, we propose a lightweight and backdrivable exoskeleton for rats, which can exert natural gait movements to all three joints in the quadrupedal posture. Fig. 1 shows an anesthetized rat being made to walk on the treadmill by the developed exoskeleton. We utilized the kinematic synergy-based exoskeletal mechanism developed in our previous work [22]. Furthermore, we configured the exoskeleton system with DD motors and flexible Bowden cables, to keep it compact, lightweight, and backdrivable while allowing sufficient area for free walking on the treadmill. This study aims to introduce a versatile robotic exoskeleton as a new platform for neurorehabilitation research using animal testing. More specifically, the proposed system aims to enable exploratory comparative studies in rats to unveil neural recovery mechanisms and design optimal exoskeleton control strategies for rehabilitation in humans.

II. System Concept

Summary of the Earlier Prototype

In our previous work, we presented a prototype consisting of two actuators that deliver assistive torques to the three hindlimb joints (hip, knee, ankle) through an underactuated mechanism with two Degrees of Freedom (2-DOF) [22]. The exoskeleton was able to replicate different gait patterns observed in nine rats [23] by exploiting the interjoint kinematic synergy of the rat during locomotion resulting in planar covariation [24].

Another design feature was the use of DD motors to facilitate safe interaction with the animal's tissues. However, the early system was heavy and large, with a weight of 282 g and dimensions of 80 mm axial thickness for one lateral unit. Such weight and size can pose significant physical stress and inertial effects on the animal.

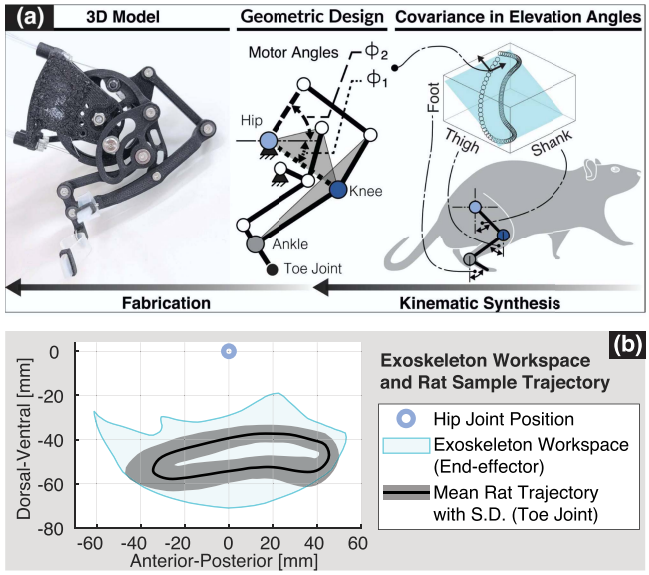

Fig. 2. **(a):** The developed bar mechanism emulates the rat's gait patterns by following the planar covariation in elevation angles. **(b):** Endeffector workspace and the mean toe joint trajectory of the reference rat sample data.

Design Criteria

In this work, we address the shortcomings of the previous prototype by relocating the actuation mechanism outside the exoskeleton and allowing the animal to relearn proper gait movements in the quadrupedal posture. We outlined the functional requirements of this exoskeleton as a research platform for gait rehabilitation:

- Gait assistance in a quadrupedal posture.
- Gait assistance for all three hindlimb joints crucial for locomotion (hip, knee, and ankle) while maintaining proper synergistic gait patterns.
- Backdrivablity to protect the animal's tissues.
- A lightweight design to minimize physical stress on the animal (1/4 body weight, based on the general device-to-user weight ratio of human exoskeletons).
- Freedom of movement for treadmill locomotion.
- A wide range of assistive forces (up to 4 N), approximately 80% of the average maximal hind-leg force of male rats [25].

III. System Overview

A. Kinematic Synergy-Based Exoskeleton

Fig. 2(a) shows the designed exoskeletal mechanism. Using kinematic synthesis, we developed a combined four-bar and five-bar mechanism with 2-DOF. The mechanism's movement is constrained to the covariance plane of limb elevation angles, replicating the innate coordinated gait patterns of rats while minimizing the number of actuators required to assist all three joints. This covariance is called kinematic synergy, seen in all intact mammals during locomotion [24]. The link parameters and geometry are the same as the previous version [22], while the mechanical design was refined, making it lighter and more

IEEE Robotics and Automation Letters (RA-L) paper, presented at ICRA 2026, Vienna, Austria. Cite as RA-L paper.

compact by replacing two link components with one slider. With this configuration, the weight of one lateral unit of the active exoskeleton became 20 g, where mechanical frames were 3D-printed with carbon-infused nylon filament (black). The initial prototype was fabricated from white polycarbonate filament shown in Figs. 4(c)–(d), 6 and 7. Fig. 2(b) shows the workspace of the end-effector. The workspace was measured on a 3D CAD system using the active contact solver. The mechanism was designed to emulate the gait patterns of several rat samples [23]. The resulting workspace overlaps the average trajectory observed in rat samples, including some deviations (20 gait cycles collected from 10 rats).

In this mechanism, there are two input cranks with angles ϕ_1 and ϕ_2, and the output joint angles $\boldsymbol{\theta}$ (hip, knee, ankle) and end-effector (toe joint) position $\boldsymbol{p}_T$ which are dependent functions of ϕ_1 and ϕ_2 (1). The detailed forward kinematics model is described in our previous work [22].

$$\boldsymbol{q} = \begin{bmatrix} \phi_1 \\ \phi_2 \end{bmatrix}, \ \boldsymbol{\theta}(\phi_1, \phi_2) = \begin{bmatrix} \theta_H \\ \theta_K \\ \theta_A \end{bmatrix}, \ \boldsymbol{p}_T(\phi_1, \phi_2) = \begin{bmatrix} x_T \\ y_T \end{bmatrix} \quad (1)$$

The relationship between the end-effector contact force and the motor torque can be derived as a static model as shown in (2), using the Jacobian matrix ((3)).

$$\begin{bmatrix} F_{xT} \\ F_{yT} \end{bmatrix} = (\boldsymbol{J}^T)^{-1} \begin{bmatrix} \tau_1 \\ \tau_2 \end{bmatrix} \quad (2)$$

$$\boldsymbol{J} = \begin{bmatrix} \partial x_T(\phi_1, \phi_2)/\partial \phi_1 & \partial x_T(\phi_1, \phi_2)/\partial \phi_2 \\ \partial y_T(\phi_1, \phi_2)/\partial \phi_1 & \partial y_T(\phi_1, \phi_2)/\partial \phi_2 \end{bmatrix} \quad (3)$$

Torque estimation based on motor current changes is feasible since the proposed system employs DD motors with a high torque coefficient. The generated torque is proportional to the motor current, described as equation (4) in a static/quasi-static condition, where K_τ is the torque coefficient, I_1 and I_2 are the currents running through the motors and τ_{cog} is the cogging torque; respectively.

$$\begin{cases} \tau_1 = K_\tau I_1, \tau_2 = K_\tau I_2 & \text{(When powered)} \\ \tau_{1,2} = \tau_{cog} & \text{(When unpowered)} \end{cases} \quad (4)$$

B. Custom Attachment Suit

A custom suit was designed to attach the exoskeleton, ensuring assistive force delivery while maintaining the animal's quadrupedal posture. Fig. 3(a) shows the suit consisting of three components: forebody suit, harness, and exo-attachment areas. The forebody suit was made of neoprene, a fabric commonly used in skin-adherent products like diving suits and sportswear. The harness was 3D printed 1.5 mm thin from carbon-infused nylon filament to afford a certain degree of compliance while being stiff enough to deliver assistive forces to the target limbs. The exoskeleton is attached to areas of the extended component from the harness allowing free position alignment on the parasagittal plane. Fig. 3(b), (d) shows the limb attachment cuffs extended from the exoskeleton, which comprises elastic silicon rubber and adjustment buckles.

Although the link parameters of the exoskeleton are fixed, the attachment suit can deliver assistance to the animal's limbs without large misalignment for the following reasons. First, the exo-attachment area allows free relocation of the exoskeleton on the parasagittal plane. Second, the limb cuffs are made of elastic silicon and do not rigidly fixate the limbs to the exoskeleton. Finally, selecting rats of similar age and sex minimizes skeletal length variation.

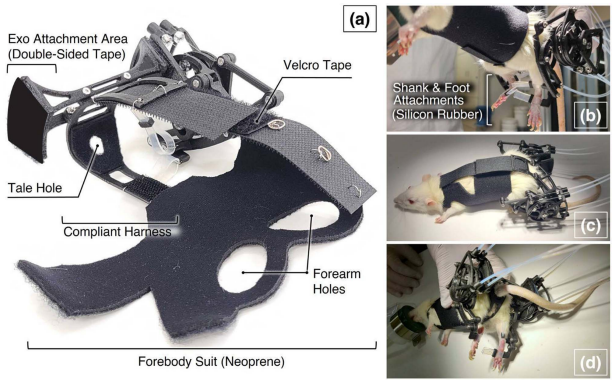

Fig. 3. Developed attachment suit for donning the exoskeleton to the animal.

C. Cable-Driven System

The developed system, shown in Fig. 4(b), consists of an actuator unit and an exoskeleton unit. The schematic of one lateral side is shown in Fig. 4(a). The two units are linked via a Bowden cable power transmission system to locate the actuators outside the exoskeleton. The actuator unit comprises four DD motors (MDS-3012-19B, Microtech Laboratory Inc.), their drivers (MC-200-7220, Microtech Laboratory Inc.), and a microcontroller (Arduino micro). The DD motors can generate up to 4 N at the end-effector (max. nominal), 80% of the maximal hind-leg force of male rats [25]. The actuation power can be increased by replacing the actuators with larger models if needed. While the larger motors increase the moment of inertia around the rotors, this impact is negligible. When a torque increases by a factor of 1.5, the motor's inertia contributes only a 2% increase to the combined inertia of the rat's hindlimb and the exoskeleton.

Since the transmission target has 2-DOF rotating in two directions (CW & CCW), there are four cables equipped in each lateral unit (Fig. 4(a)). We designed the cables to form curves relative to the animal's location to allow a certain degree of freedom for the animal to move back and forth and sideways. Here, we defined the inner cable's curve as an arc with constant curvature and the outer cable's curve as a combination of an arc and two symmetric straight lines, which also helps minimize friction. Fig. 4(c)–(d) shows the designed Bowden cable mechanism. We defined the working operation range as 300 mm in the anterior-posterior direction to provide half the lane distance of a rodent treadmill, and 100 mm in the mediolateral direction. The Bowden cables were fabricated from stainless steel wires for the pulling cables and PTFE tubes for the housing to minimize friction. Hollow bolts were attached to the tube ends to allow precise tension adjustment. Attaching the exoskeleton to the cables added 5–10 g of downforce due to the cable housing, depending on curvature. When the exoskeleton was assembled with the cables and the suit, the total weight of the exoskeleton unit became approximately 80 g. Since the weight of the subject animal (adult female Sprague Dawley rat) is 300–350 g, the developed exoskeleton should be lightweight enough as a wearable gait assistive robot. Table I provides a comparison between the developed system and existing systems in the field, based on

IEEE Robotics and Automation Letters (RA-L) paper, presented at ICRA 2026, Vienna, Austria. Cite as RA-L paper.

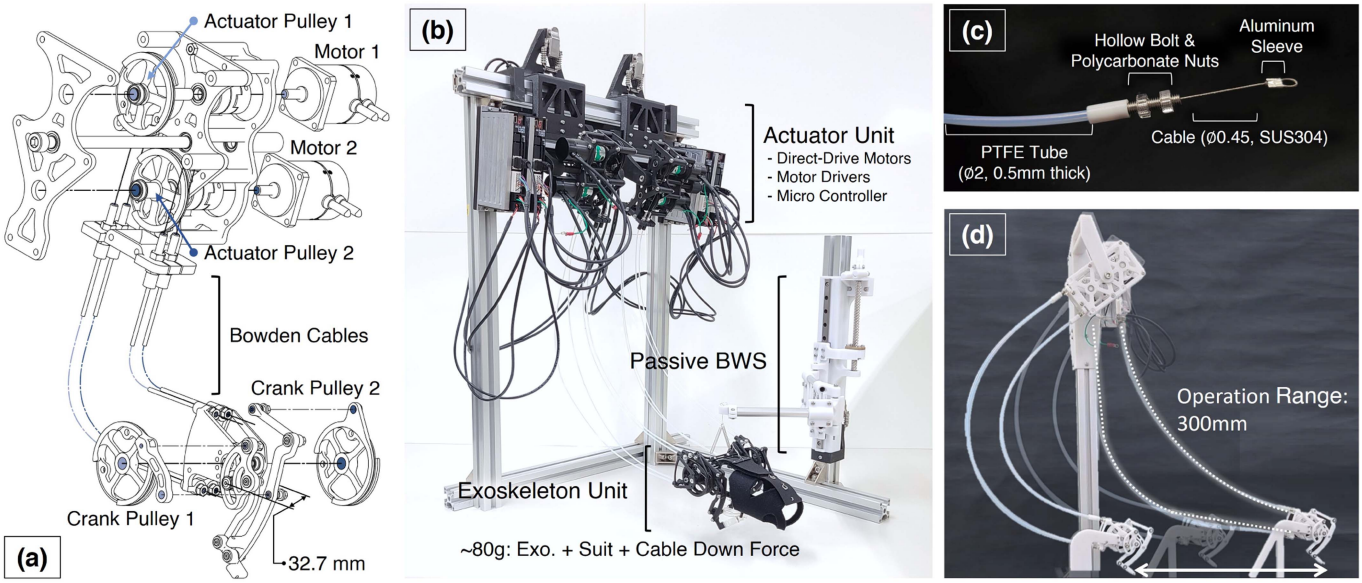

Fig. 4. Developed cable-driven system transmitting the DD motor's backdrivable actuation from the actuator unit to the exoskeleton unit through the Bowden cables. **(a):** a mechanical design schematic. **(b):** a system overview. **(c):** the developed Bowden cable. **(d):** three different locations of the exoskeleton relative to the actuator unit and the corresponding cable deformation.

TABLE I
SPECIFICATION COMPARISON

	Assist Type	Weight	Assisted Joints	Assist Post.	Safety	Max. Force
This Work	Phy.	80 g	3	Quad.	BD	4 N
Song[19]	Phy.	75 g	2	Quad.	BD	2 N
Florez[17]	Phy.	150 g	2	Up.	Comp.	5 N
Chang[18]	Phy.	-	2	Up.	Comp.	1.6 N
Nessler[16]	Phy.	Gr.	2	Up.	BD	1.5 N
Anopas[20]	Phy.	Gr.	2	Quad.	None	-
Dominici[12]	SCS	-	2	Up.	Elec.	-
Xi[14]	EMS	-	3	Up.	Elec.	-

Phy.: Physical, Quad.: Quadrupedal, Up.: Upright, Gr.: Grounded
BD: Backdrivable, Comp.: Compliant, Elec.: Electrical

the criteria outlined in this study; considering the weight of the active exoskeleton worn by the animal.

D. Trajectory Tracking Control System

We implemented a feedforward trajectory tracking control system that utilizes the rotary encoders embedded within the motors. Since no sensors are attached directly to the exoskeleton, this work does not account for potential effects of clearance or elasticity in the mechanism, including the cable power transmission. By neglecting these mechanical errors, the actuator unit focuses on controlling the motors to follow the target positions, while the cable transmission system transfers the motor actuation to the exoskeleton.

The control system operates as follows: A microcontroller generates a predefined trajectory based on the desired gait speed and sends target position commands to the motor drivers at a frequency of 100 Hz. The motor drivers then use PID control at 50 kHz to closely track the target positions. The PID gains were empirically tuned under conditions where the only load was the exoskeletal mechanism. For data logging, the motor drivers relay the angular positions and the applied currents back to the microcontroller.

IV. EXPERIMENTAL EVALUATION

The experimental evaluation focused on verifying four key aspects of the exoskeleton: kinematic performance, backdrivability, cable transmission efficiency, and feasibility of gait assistance under *in vivo* conditions. The experiments are described below as: trajectory tracking evaluation (no-load), backdrivability evaluation, load sensitivity evaluation, and gait assistance test *in vivo*. The *in vivo* experiment was performed under the guidelines for the proper conduct of animal experiments and was approved by the Animal Research Committee of the University of Tsukuba (approval number 24-412).

A. Trajectory Tracking Evaluation (No-Load)

The kinematic performance of the developed exoskeleton was evaluated by comparing its trajectories to the reference sample trajectories of an intact rat [23]. The evaluation is based on the joint angles, elevation angle planar covariation, and the toe joint (end-effector) position.

During the trials, the exoskeleton was driven to generate a gait pattern via PID position control (III-D). The joint angles were extracted from video data recorded at 120 Hz for 10 cycles. The collected data was then averaged and the toe joint positions were calculated from the averaged joint angles. The reference trajectories in Fig. III-D(a)–(b) were calculated by forward kinematics using the control commands to visualize the mechanical errors.

As shown in Fig. 5(a)–(b), the system effectively replicated the rat's trajectory with minimal deviation, demonstrating compatibility with the new cable transmission system. The error in the ankle angle observed around 40% of the gait cycle highlights a limitation of the mechanism, which arises from the need to accommodate a variety of gait patterns. Principal component

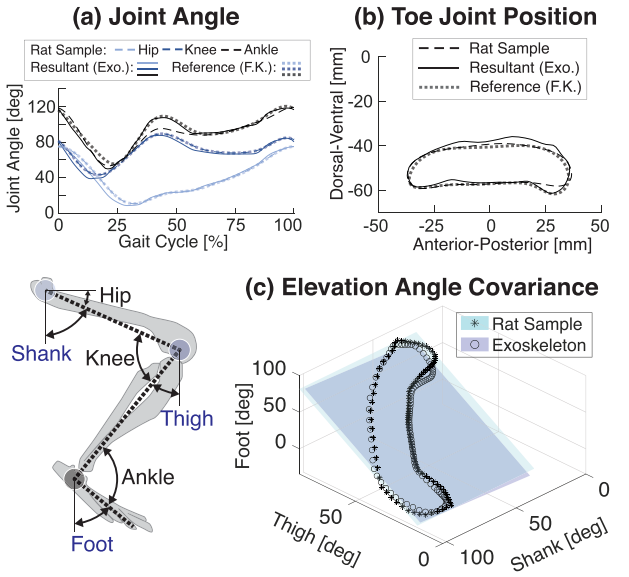

Fig. 5. Experimental results from the trajectory tracking evaluation comparing to an intact rat sample data [23]. **(a):** Joint angles were extracted from the recorded video data, being compared to the rat sample data and the reference trajectories generated by the exoskeleton's forward kinematcs. The deviation is not shown as it is significantly small. **(b):** Toe joint trajectories are calculated with forward kinematics. **(c):** Limb elevation angle covariance planes (interjoint coordination) were generated based on principal component vectors of limb angle data.

analysis (PCA) was performed on the resulting limb elevation angles to quantify interjoint coordination (Fig. 5(c)). The difference in the inclination of the covariance planes between the rat sample and the mechanism was minimal, with the inner product of the two PC3 vectors being 0.98 (1 max.). This result indicates that the synergistic gait pattern was accurately replicated.

B. Backdrivability Evaluation

The backdrivability of the developed exoskeleton was evaluated by applying external forces exceeding the actuators' output. This experiment aims to evaluate the feasibility of implementing an assist-as-needed condition, ensuring that the robot provides gait assistance without fully restricting the animal's movement. The top figure in Fig. 6 shows the experimental setup, where the end-effector is connected to a force gauge through a flexible stainless steel cable.

The experiment was performed in two conditions: powered and unpowered. For each condition, the trial was conducted only once for clarity since there was no significant difference during repetitions. In the powered condition, a current limit of 1.5 A was applied to the driver circuit, which can generate approximately 2 N at the end-effector, being 40% of the maximal force generated by the hind extremities of intact male rats [25]. During the powered trial, the exoskeleton was commanded to stay at one position with PID control while manually being pulled back by the force gauge. In the unpowered trial, the exoskeleton was only recording the joint angles. The generated force was calculated using the static model (Section III-A), and the motor current was recorded from the motor driver. The backdriving force was applied consistently over a 3-second duration because the static model does not account for dynamic properties.

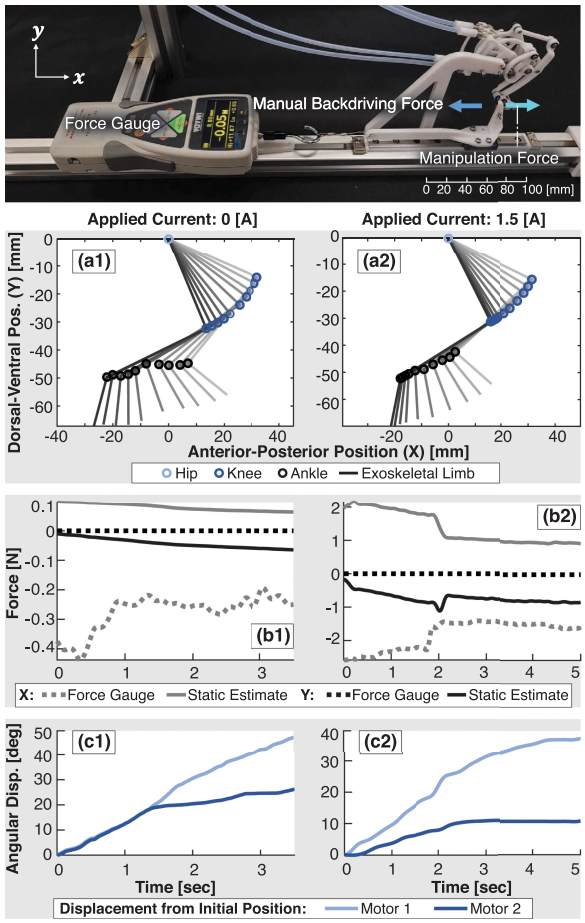

Fig. 6. **Top image:** the experimental setup for backdrivability evaluation. The end effector is pulled horizontally using a force gauge while the motors are unpowered, and while being commanded to maintain a forward position of the leg. **Graphs:** Backdrivability evaluation results for unpowered (0 A) and powered condition (1.5 A current limit). **(a1-2):** The limb movement calculated from motor angles at 0 A and 1.5 A. **(b1-2):** The backdriving force measured by the force gauge and the generated force estimated by the motor currents and angular positions using the static model at 0 A and 1.5 A. **(c1-2):** The angular displacement of the motors from the initial position at 0 A and 1.5 A.

The results in Fig. 6 confirm high backdrivability under both powered and unpowered conditions. The exoskeleton was pulled backward (a1-a2) with measured forces aligning with the expected static model predictions (b1-b2), and both the motors were successfully backdriven (c1-c2). The end-effector moved diagonally despite the horizontally applied force. This error could be due to the slack of the pulling wire and the friction from the mechanical components. Regarding the generated force, there was a 0.4-0.44 N difference observed when comparing the measured and generated force as shown in Fig. 6(c1)–(c2). The deviation towards the vertical axis is also seen in the force profile. For the powered condition, the maximum horizontal backdriving force required was 2.6 N, whereas the force generated by the motors was approximately 2.2 N. As for the unpowered condition, the maximum horizontal backdriving force required was 0.45 N, whereas the force generated by the motors' cogging was approximately 0.1 N. When considering the rat's maximal hind-leg force, 5 N [25], this exoskeleton should be backdrivable for the animal. The observed 0.4–0.44 N deviation highlights

IEEE Robotics and Automation Letters (RA-L) paper, presented at ICRA 2026, Vienna, Austria. Cite as RA-L paper.

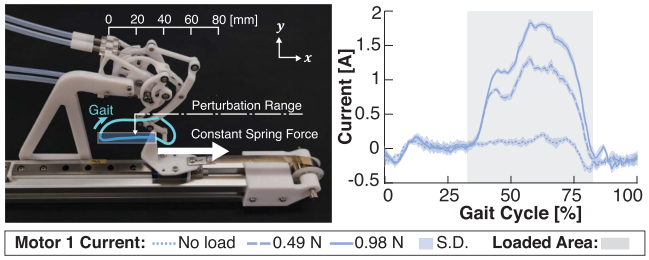

Fig. 7. **Photo:** Experimental setup for load sensitivity evaluation: the robot actuates a constant spring-loaded sliding mechanism, where the spring is constrained to only exert a horizontal force. **Graph:** Result of load sensitivity evaluation. The dotted and sold lines represent the resultant currents of motor 1 at different load conditions (0, 0.49 and 0.98 N). The loaded phase in the cycle is shaded in gray.

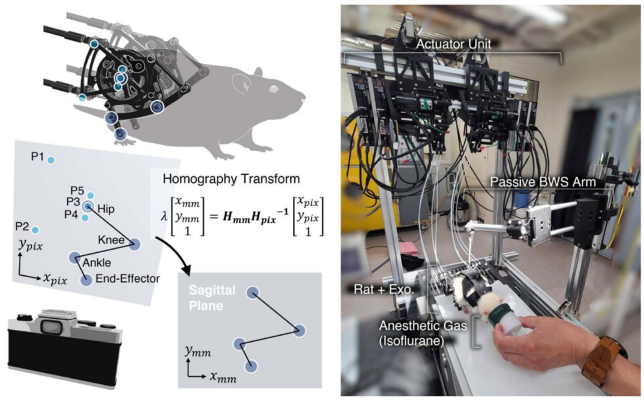

Fig. 8. Experimental setup for the *in vivo* feasibility test. **Right:** An anesthetized rat wearing the developed exoskeleton while being suspended by the passive body weight support arm on a rodent treadmill. **Left:** A camera device recorded the exoskeleton's movement.

minor frictional effects but remains within acceptable limits for assist-as-needed protocols.

C. *Load Sensitivity Evaluation*

This experiment was conducted to observe motor current behavior under varying load conditions. Given the system's complexity, it is unclear how effectively external forces are transmitted to the actuators and reflected in the motor's electric current.

The experiment involved applying a constant horizontal cyclic force to the end-effector, replicating the scenario where the exoskeleton generates propulsion force on a treadmill. The left image in Fig. 7 illustrates the experimental setup. During the experiment, the exoskeleton operated in a gait cycle while a constant spring force (0.49 N and 0.98 N) was applied in the opposing direction at the end-effector. The exoskeleton's gait pattern was driven by PID position control (III-D), and motor current data was collected at a sampling rate of 200 Hz over 10 gait cycles. These measurements were then averaged. Motor 1 was selected for current measurement due to its dominant geometric role in exerting horizontal forces.

Initially, the exoskeleton was tested at different positions within the Bowden cable's operational range, and the results showed no significant differences. Consequently, the experiment was performed at a fixed position. We also tested it with different PID gains and the current profiles seemed sensitive to the proportional gain, which could be due to the differences in response time, modifying the dynamic variables. The results, presented in Fig. 7, indicate that the system successfully transmits external forces to the motor, producing significant changes in current.

D. *Gait Assistance Test* in vivo

A preliminary driving test on an anesthetized rat was performed to confirm the feasibility of the proposed gait assistance method with the exoskeleton. The subject animal was a female rat with a body weight of 340 g.

Fig. 8 shows the experimental setup consisting of the exoskeleton system, a passive body weight support (BWS) arm, a rodent treadmill, an anesthetic vaporizer system for inhaled anesthesia (face mask shown only), and a camera device (not shown in the picture). The animal was supported by a passive BWS arm connected through a wire and a tension spring. The supported weight was manually adjusted to maintain adequate contact between the toes and the treadmill belt. The animal was subjected to anesthetic gas (2–3% isoflurane) to keep the limbs flaccid throughout the experiment including attaching/detaching the exoskeleton. The motor drivers were configured with a current limit of 1.5 A to ensure safety and prevent potential tissue damage to the animal. A video was recorded from the side of the treadmill and tracked the motions of the essential points on the exoskeleton as shown in Fig. 8. It was not viable to track the actual joints of the animal due to the optical occlusion from the exoskeleton. During the experiment, the flaccid animal was moved by the exoskeleton to walk on the treadmill with its hindlimbs at 1.3 Hz which is equivalent to 115 mm/s of locomotion.

Fig. 9 shows a time-series picture of the anesthetized rat's gait cycle over the treadmill while using the exoskeleton. As shown in the photos, the exoskeleton successfully imposed rhythmic gait patterns on the flaccid limbs of the anesthetized rat. Fig. 10 shows the kinematics extracted from the recorded video data. The visualized limb segment movement was estimated using the measured exoskeleton angles, demonstrating successful limb motion to produce stepping (Fig. 10(c)). In Fig. 10(a), significant amplitude errors in the joint angles, compared to the no-load trajectories, were observed due to the current limit and the mechanical impedance of the rat's musculoskeletal system. Despite these errors, the resulting limb motion exhibited strong interjoint coordination. This is evidenced by 99% of variance being explained by two principal components in the covariance plane (Fig. 10(b)).

V. Discussion

A. *Limb Coordination and Posture*

The proposed exoskeleton was designed to maintain appropriate interjoint coordination and the natural quadrupedal gait posture. The experimental results validated both objectives. The trajectory tracking evaluation experiment (IV-A) showed the robot to retain the limb coordination of the bar mechanism [22] despite the added cable transmission system. Further, the *in vivo* test with the anesthetized rat (IV-D) confirmed that the exoskeleton could achieve the intended limb coordination and gait posture. Preliminary tests without ankle joint assistance (not shown) revealed that the flaccid foot was dragged by the treadmill belt, underscoring the importance of ankle assistance in

IEEE Robotics and Automation Letters (RA-L) paper, presented at ICRA 2026, Vienna, Austria. Cite as RA-L paper.

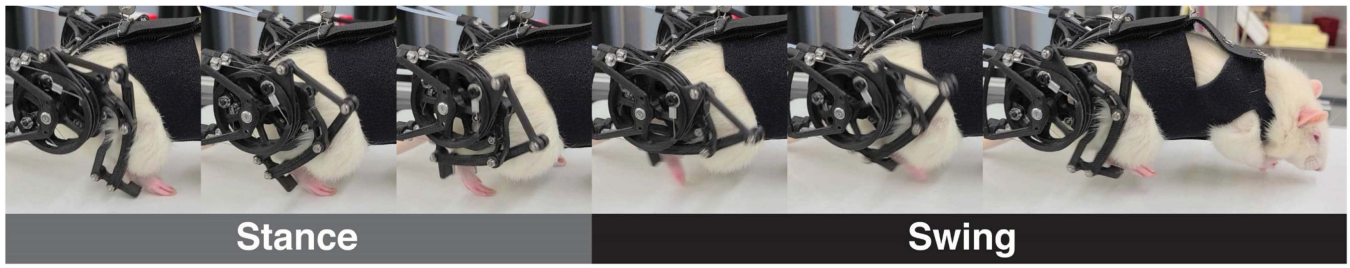

Fig. 9. Time series photos of the anesthetized rat being made to walk by the proposed exoskeleton.

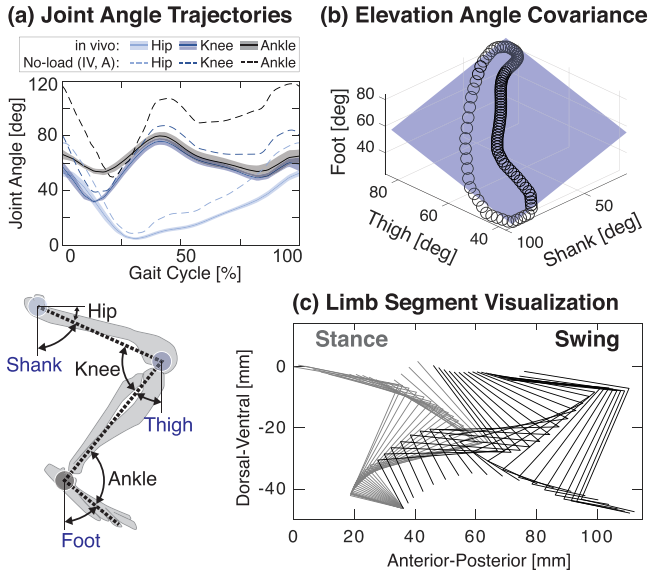

Fig. 10. Experimental result of the *in vivo* feasibility test. **(a):** Joint angles were extracted from the tracked positions of the exoskeleton. **(b):** Elevation angle covariance plane (interjoint coordination) was generated based on the principal component vectors. **(c):** Limb segment movements are visualized by forward kinematics using the joint angles.

quadrupedal posture. Other existing systems tested quadrupedal gait assistance only on fully intact animals [19] or with locked ankles [20]. To our knowledge, this is the first system to actively assist all three hindlimb joints in a quadrupedal posture.

While this study focuses on rats, their locomotor system shares key neural mechanisms with humans. Adaptive locomotion in mammals involves conserved neural strategies integrating nervous system inputs, body dynamics, and environmental feedback [26]. Humans also retain elements of quadrupedal control, such as inter-limb coordination and reflex pathways, reflecting the evolutionary continuity of locomotor control across species [27]. These shared mechanisms make rats a valuable model for studying neural principles relevant to human rehabilitation.

B. Mobility Restrictions

Increasing the assist power usually incurs an increase in the exoskeleton's weight. The proposed cable-driven solution enables the lightest yet most powerful exoskeleton among the existing systems (Table I), minimizing the inertial effect on the animal while delivering substantial assistive force.

The cable transmission limits the locomotion freedom to a treadmill. While untethered robotic exoskeletons are available for humans, current rehabilitation systems for rats typically confine movement to fixed positions on the treadmill [16], [17], [20]. Few studies have explored overground locomotion [19], but even these systems require tethering for BWS and electric power transmission. In comparison, the robot proposed here allows a degree of freedom on a treadmill stretching 300 mm in the anterior-posterior direction and 100 mm in the mediolateral direction. While a fully untethered solution is not viable given the current actuator technology, the authors consider the proposed design to be a suitable compromise between assistive force and mobility restrictions.

C. Backdrivability

The proposed exoskeleton showed intrinsic backdrivability without feedback control when the motors were powered and not powered, presenting approximately 0.44 N added by friction (IV-B). This frictional force is one-tenth of the rat's maximal hind-leg force, 5 N [25], allowing various experimental protocols by actively assisting/resisting the animal's movements while only exerting the required force without large static friction. Notably, during the feasibility test, the animal pushed back against the assistive force exerted by the exoskeleton when we awakened it to observe the behavior. The reduced friction in the system was further evidenced by motor current profiles during the load sensitivity evaluation (IV-C). This experiment highlighted the potential of the DD motors to function as internal sensors within this system. By accounting for the mechanical system's dynamics, it may be possible to implement a force feedback control system using motor current data in combination with other state variables.

Limitations

The limitations of this work include the tested control strategies and the tested physiological condition and size variation of the subject animal.

This work did not implement a closed-loop feedback control strategy. Therefore, the animals' body properties such as body weight and the mechanical impedance of their joints were not considered. In future studies, we will explore more sophisticated sensing and control strategies, the effective range of assistive forces, and the range of kinematics achievable with the system. In addition, we observed that the motor's driving currents are significantly influenced by the PID gains under dynamic conditions. Therefore, when utilizing DD motors as torque sensors, it is essential to determine the optimal PID gains for that usage.

In this work, we only tested the exoskeleton's feasibility on an anesthetized rat. When using rats paralyzed by neurological injuries, musculoskeletal conditions may differ depending on the

IEEE Robotics and Automation Letters (RA-L) paper, presented at ICRA 2026, Vienna, Austria. Cite as RA-L paper.

type of paralysis. In particular, the ankle manipulation achieved by the sets of two couplings might trigger the foot withdrawal reflex in non-anesthetized animals, which can disturb the desired gait assistance. Thus, we need to investigate the feasibility and appropriate use of the exoskeleton on paralysis-induced rats in the future. Furthermore, the device's adaptability across different animal sizes was not assessed. Although laboratory rats have minimal size variation, the device's versatility should be investigated.

VI. Conclusion

In this letter, we presented a robotic exoskeleton with mechanically implemented kinematic synergy designed for rehabilitation studies in rats. The system provides assistance to all three hindlimb joints (hip, knee and ankle), which are critical for natural quadrupedal locomotion, while maintaining proper inter-joint coordination through the proposed 2-DOF synergy-based exoskeletal mechanism. By relocating the actuation source outside the exoskeletal structure, the design achieved a compact and lightweight configuration, preserving the backdrivable properties of the DD motors via the proposed power transmission system.

Future investigations will focus on implementing advanced control strategies (e.g., assist-as-needed control) to study recovery differences under carefully controlled experimental environments *in vivo*. The ultimate goal of this study is to establish a versatile experimental platform for rats, contributing to foundational studies in neurorehabilitation.

References

[1] S. Di, W. Zhang, W. Zhang, and X. Ding, "A review on lower limb rehabilitation exoskeleton robots," *Chin. J. Mech. Eng.*, vol. 32, no. 1, 2019, Art. no. 74.

[2] Y.-N. Chen, Y.-N. Wu, and B.-S. Yang, "The neuromuscular control for lower limb exoskeleton- a 50-year perspective," *J. Biomech.*, vol. 158, 2023, Art. no. 111738.

[3] J. Veldema and P. Jansen, "Resistance training in stroke rehabilitation: Systematic review and meta-analysis," *Clin. Rehabil.*, vol. 34, no. 9, pp. 1173–1197, 2020.

[4] H. Lee, J. Park, and T.-W. Kim, "Comparisons between Locomat and Walkbot robotic gait training regarding balance and lower extremity function among non-ambulatory chronic acquired brain injury survivors," *Medicine*, vol. 100, 2021, Art. no. e25125.

[5] Y. Zhang et al., "Exoskeleton rehabilitation robot training for balance and lower limb function in sub-acute stroke patients: A pilot, randomized controlled trial," *J. NeuroEngineering Rehabil.*, vol. 21, 2024, Art. no. 98.

[6] G. Kwakkel, B. Kollen, and H. Krebs, "Effects of robot-assisted therapy on upper limb recovery after stroke: A systematic review," *Neurorehabilitation Neural Repair*, vol. 22, no. 2, pp. 111–121, 2007.

[7] D. Louie et al., "Efficacy of an exoskeleton-based physical therapy program for non-ambulatory patients during subacute stroke rehabilitation: A randomized controlled trial," *J. NeuroEngineering Rehabil.*, vol. 18, 2021, Art. no. 149.

[8] H. Rodgers et al., "Robot assisted training for the upper limb after stroke (RATULS): A multicentre randomised controlled trial," *Lancet*, vol. 394, no. 10192, pp. 51–62, 2019.

[9] F. Baronchelli, C. Zucchella, M. Serrao, D. Intiso, and M. Bartolo, "The effect of robotic assisted gait training with lokomat on balance control after stroke: Systematic review and meta-analysis," *Front. Neurol.*, vol. 12, 2021, Art. no. 661815.

[10] A. Rodríguez-Fernández, J. Lobo-Prat, and J. Font-Llagunes, "Systematic review on wearable lower-limb exoskeletons for gait training in neuromuscular impairments," *J. Neuroengineering Rehabil.*, vol. 18, 2020, Art. no. 22.

[11] J. Cao, S. Q. Xie, R. Das, and G. L. Zhu, "Control strategies for effective robot assisted gait rehabilitation: The state of art and future prospects," *Med. Eng. Phys.*, vol. 36, no. 12, pp. 1555–1566, 2014.

[12] N. Dominici et al., "Versatile robotic interface to evaluate, enable and train locomotion and balance after neuromotor disorders," *Nature Med.*, vol. 18, pp. 1142–1147, 2012.

[13] M. Bonizzato et al., "Multi-pronged neuromodulation intervention engages the residual motor circuitry to facilitate walking in a rat model of spinal cord injury," *Nature Commun.*, vol. 12, no. 1, 2021, Art. no. 1925.

[14] P. Xi, Q. Yao, Y. Liu, J. He, R. Tang, and Y. Lang, "Biomimetic peripheral nerve stimulation promotes the rat hindlimb motion modulation in stepping: An experimental analysis," *Cyborg Bionic Syst.*, vol. 5, 2024, Art. no. 0131.

[15] J. Nessler, K. Minakata, K. Sharp, and D. Reinkensmeyer, "Robot-assisted hindlimb extension increases the probability of swing initiation during treadmill walking by spinal cord contused rats," *J. Neurosci. Methods*, vol. 159, pp. 66–77, 2007.

[16] M. Leblanc, M. Soucy, M. Moustafa-Bayoumi, D. Soto, and J. Nessler, "Effect of robotic gait training on muscle and bone characteristics in spinal cord transected rats," *J. Orthopaedic Res. : Official Publication Orthopaedic Res. Soc.*, vol. 42, pp. 1519–1526, 2024.

[17] J. M. Florez et al., "Rehabilitative soft exoskeleton for rodents," *IEEE Trans. Neural Syst. Rehabil. Eng.*, vol. 25, no. 2, pp. 107–118, Feb. 2017.

[18] S.-Y. Chang et al., "Design of small-size pouch motors for rat gait rehabilitation device," in *Proc. 37th Annu. Int. Conf. IEEE Eng. Med. Biol. Soc.*, 2015, pp. 4578–4581.

[19] Y. S. Song and N. Hogan, "A novel interactive exoskeletal robot for overground locomotion studies in rats," *IEEE Trans. Neural Syst. Rehabil. Eng.*, vol. 23, no. 4, pp. 591–599, Jul. 2015.

[20] D. Anopas, S. Y. Chew, J. Lin, S. K. Wee, T. P. Er, and W. T. Ang, "A developmental rehabilitation robotic system for a rat with complete thoracic spinal cord injury in quadruped posture," *IEEE Robot. Automat. Lett.*, vol. 3, no. 3, pp. 2109–2115, Jul. 2018.

[21] E. Andrada et al., "Biomechanical analyses of rat locomotion during walking and climbing as a base for the design and construction of climbing robots," *WIT Trans. Ecol. Environ.*, vol. 138, pp. 165–177, 2010.

[22] T. Miyamoto, L. Ccorimanya, M. Hassan, S. Puentes, and K. Suzuki, "Joint synergy-based rehabilitative exoskeleton for rodents," in *Proc. 2022 IEEE/ASME Int. Conf. Adv. Intell. Mechatron.*, 2022, pp. 1225–1230.

[23] K. Deng et al., "Neuromechanical model of rat hindlimb walking with two-layer CPGs," *Biomimetics*, vol. 4, 2019, Art. no. 21.

[24] G. Catavitello, Y. Ivanenko, and F. Lacquaniti, "A kinematic synergy for terrestrial locomotion shared by mammals and birds," *eLife*, vol. 7, Oct. 2018, Art. no. e38190.

[25] A. Iwata, S. Fuchioka, K. Hiraoka, M. Masuhara, and K. Kami, "Characteristics of locomotion, muscle strength, and muscle tissue in regenerating rat skeletal muscles," *Muscle Nerve*, vol. 41, pp. 694–701, 2010.

[26] H. Chiel, L. Ting, O. Ekeberg, and M. Hartmann, "The brain in its body: Motor control and sensing in a biomechanical context," *J. Neurosci.*, vol. 29, no. 41, pp. 12807–12814, 2009.

[27] E. Zehr et al., "Neuromechanical interactions between the limbs during human locomotion: An evolutionary perspective with translation to rehabilitation," *Exp. Brain Res.*, vol. 234, pp. 3059–3081, 2016.